European Journal of Control 68 (2022) 100679

Contents lists available at ScienceDirect

European Journal of Control

journal homepage: www.elsevier.com/locate/ejcon

Maximum-distance race strategies for a fully electric endurance race car☆

Jorn van Kampen[a,*], Thomas Herrmann[b], Mauro Salazar[a]

[a] Control Systems Technology Group, Eindhoven University of Technology, 5600 MB Eindhoven, The Netherlands
[b] Institute of Automotive Technology, Department of Mechanical Engineering, Technical University of Munich (TUM), Germany

ARTICLE INFO

Article history:
Received 14 April 2022
Accepted 6 June 2022
Available online 17 June 2022

Recommended by Prof. T Parisini

Keywords:
Electric vehicles
Endurance racing
Optimal control
Optimization
Race strategy

ABSTRACT

This paper presents a bi-level optimization framework to compute the maximum-distance stint and charging strategies for a fully electric endurance race car. Thereby, the lower level computes the minimum-stint-time Powertrain Operation (PO) for a given battery energy budget and stint length, whilst the upper level leverages that information to jointly optimize the stint length, charge time and number of pit stops, in order to maximize the driven distance in the course of a fixed-time endurance race. Specifically, we first extend a convex lap time optimization framework to capture multiple laps and force-based electric motor models, and use it to create a map linking the charge time and stint length to the achievable stint time. Second, we leverage the map to frame the maximum-race-distance problem as a mixed-integer second order conic program that can be efficiently solved to the global optimum with off-the-shelf optimization algorithms. Finally, we showcase our framework on a 6 h race around the Zandvoort circuit. Our results show that a flat-out strategy can be extremely detrimental, and that, compared to when the stints are optimized for a fixed number of pit stops, jointly optimizing the stints and number of pit stops can increase the driven distance of several laps.

1. Introduction

The electrification of race cars has been increasing in popularity over the last years, owing to the adven of hybrid electric Formula 1 cars and Le Mans Hypercars, and battery electric vehicles in Formula E. In a setting where every millisecond counts, it is of paramount importance to profit the most of the energy stored on-board via optimized Energy Management Strategy (EMS). In this context, the possibility of recharging the battery in the course of the race further complicates the problem, requiring race engineers to strike the best trade-off between reducing consumptions and pit-stops at the cost of lap-time, or driving faster with more pit-stops. This conflict becomes particularly imminent in endurance racing, where the objective is to maximize the driven distance in a fixed amount of time, which can range up to 24h [1]. In this setting, the car has to be strategically recharged during pit stops in order to maintain a competitive performance, maximizing the distance driven. This calls for algorithms to compute the maximum-distance race strategies that provide the number of pit stops during the race, the number of laps driven per stint (referred to as stint lengths) and charge time (which is directly correlated to charge energy), whilst accounting for the optimal energy management strategies and Powertrain Operation (PO). Against this backdrop, this paper presents a bi-level optimization framework to compute the maximum-distance race strategies with global optimality guarantees.

1.0.1. Related literature

This work pertains to two main research streams: single-lap optimization of the EMSs jointly with the vehicle trajectory or for a given race line, and full-race optimization via simulations.

Several authors optimized the minimum-lap-time race line for a single race lap using both direct and indirect optimization methods [2–8]. Some of these studies also include a maximum energy consumption per lap to approach racing conditions [9]. Similar approaches extend the minimum-lap-time problems to minimum-race-time problems. They consider temperature dynamics, and optimize for multiple consecutive race laps to enable a variable amount of energy consumed per lap, but formulate the optimization problem in space domain for an a priori known number of

☆ Recommended by T Parisini

* Corresponding author.
E-mail address: j.h.e.v.kampen@student.tue.nl (J. van Kampen).

https://doi.org/10.1016/j.ejcon.2022.100679

laps [10,11]. Finally, considering the race line to be fixed, multi-lap EMSs are optimized, leveraging nonlinear optimization techniques [12] or artificial neural networks [13]. However, these papers lack global optimality guarantees.

Against this backdrop, assuming the race line to be available in the form of a maximum speed profile, convex optimization has been successfully leveraged to compute the globally optimal EMSs for hybrid and fully electric race vehicles [14,15], also including gear shift strategies [16], different transmission technologies [17] and thermal limitations [18]. Yet these methods are focused on single-lap problems and do not capture pit-stops and recharging processes.

A final relevant research stream involves race simulations, in which entire races are optimized on a per lap basis [19,20]. However, these studies mainly focus on optimal tire strategies by modeling their degradation as a lap time increase and do not capture the charging and PO strategies. In conclusion, to the best of the authors' knowledge, there are no methods specifically focusing on race strategies in endurance scenarios, whereby the PO within a stint and the stints themselves are jointly optimized.

1.0.2. Statement of contributions

This paper presents a bi-level mixed-integer convex optimization framework to efficiently compute the globally optimal, maximum-distance endurance race strategies and the corresponding PO in the individual stints. Our low-level algorithm computes the optimal stint time for a given number of laps and different levels of recharged battery energy. To preserve convexity, we describe the EM efficiency by using speed-dependent in- and output forces. Subsequently, we fit the relationship between the stint length, the charged energy, and the achievable stint time as a second-order conic constraint, which we leverage in the high-level algorithm. Thereby we frame the maximum-distance race problem as a mixed-integer second-order conic program which jointly optimizes the stint length, the charge time—i.e., the charge energy—and the number of pit stops. The resulting problem can be rapidly solved with off-the-shelf numerical solvers with global optimality guarantees. Finally, we showcase our framework on the Zandvoort circuit for the vehicle shown in Fig. 1, highlighting the importance of jointly optimizing the number of pit stops with the stint lengths and charging strategies.

1.0.3. Organization

The remainder of this paper is structured as follows: Section 2 presents the minimum-stint-time control problem, after which Section 3 frames the maximum-race-distance control problem. We showcase our framework for a 6 h race in Section 5. Finally, Section 6 draws the conclusions and provides an outlook on future research.

2. Low-level stint optimization

This section illustrates the minimum-stint-time control problem in space domain, since minimizing the stint time given a fixed distance represents the dual problem of maximizing distance within a fixed time period. We extend an existing convex framework [17] to allow multi-lap optimization, whilst improving the EM model accuracy by considering a pre-defined fixed-gear transmission ratio. Thereby we separate the EM and inverter model to allow future extensions to temperature models. From the time-optimal control problem, we obtain the minimum stint time for a given stint length and available battery energy (which can be equivalently expressed in terms of charging time).

Fig. 2 shows a schematic representation of the powertrain topology of the electric race car. The EM propels the rear wheels through a fixed Final Drive (FD), while receiving energy from the battery pack via the inverter. As with most electric vehicles, the EM can also operate as a generator, thus we account for a bi-directional energy flow between the battery and the wheels. In addition, we consider auxiliary components that are powered from the main battery as a uni-directional energy flow.

Fig. 1. InMotion's fully electric endurance race car.

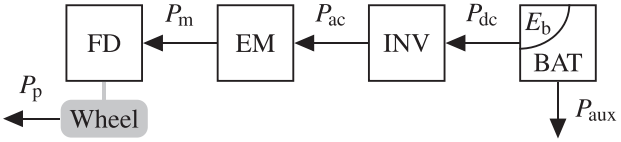

Fig. 2. Schematic layout of the electric race car powertrain topology consisting of a battery (BAT), inverter (INV), electric machine (EM) and final drive (FD). The arrows indicate positive power flows of the auxiliary power P_{aux}, the electrical inverter power P_{dc}, the electrical electric motor(EM) input power P_{ac} and mechanical output power P_m, and the propulsion power P_p.

In reality, the driver controls the EM torque through the accelerator pedal and as such we define the mechanical EM power P_m as the input variable. As state variables, we choose the battery energy E_b and the kinetic energy of the vehicle E_{kin}. The remaining energy flows between the powertrain components are the propulsion power P_p, electrical EM power P_{ac}, electrical inverter power P_{dc} and auxiliary supply P_{aux}. Since we formulate the control problem in space domain, we ultimately define the model in terms of forces rather than power. Thus we divide power by the vehicle velocity, since the space-derivative of energy is defined with respect to the vehicle.

2.1. Objective and longitudinal dynamics

In racing, the objective is to minimize the lap times over the entire race. Since we only consider a stint in the low-level control problem, the objective is to minimize the stint time t_{stint}, which is defined as

$$\min t_{stint} = \min \int_0^{S_{stint}} \frac{dt}{ds}(s)\, ds, \tag{1}$$

where S_{stint} is the stint length in terms of distance and $\frac{dt}{ds}(s)$ is the lethargy, which is the inverse of the vehicle velocity $v(s) \geq 0$. To implement the lethargy as a convex constraint, we define

$$\frac{dt}{ds}(s) \geq \frac{1}{v(s)}, \tag{2}$$

which is a convex relaxation that holds with equality in case of an optimal solution [14].

Since the goal of this paper is to study the optimal race strategy and PO rather than studying the effect of vehicle dynamics, we model the vehicle as a point mass, for which the longitudinal dynamics are written as

$$\frac{d}{ds}E_{kin}(s) = F_p(s) - F_d(s) - F_{brake}(s), \tag{3}$$

where $F_p(s)$ is the propulsion force, $F_d(s)$ is the drag force and $F_{brake}(s)$ is the force from the mechanical brakes. The drag force is defined as the sum of the aerodynamic drag, the rolling resistance and the gravitational force as

$$F_{\mathrm{d}}(s) = \frac{c_{\mathrm{d}} \cdot A_{\mathrm{f}} \cdot \rho}{m_{\mathrm{tot}}} \cdot E_{\mathrm{kin}}(s) + c_{\mathrm{r}} \cdot (m_{\mathrm{tot}} \cdot g \cdot \cos(\theta(s)) + F_{\mathrm{down}}(s)) + m_{\mathrm{tot}} \cdot g \cdot \sin(\theta(s)), \quad (4)$$

where m_{tot} is the total mass of the vehicle, c_{d} is the air drag coefficient, A_{f} is the frontal area of the vehicle, ρ is the air density, c_{r} is the rolling resistance coefficient, g is the gravitational constant, $\theta(s)$ is the inclination of the track and $F_{\mathrm{down}}(s)$ is the aerodynamic downforce defined by

$$F_{\mathrm{down}}(s) = \frac{c_{\mathrm{l}} \cdot A_{\mathrm{f}} \cdot \rho}{m_{\mathrm{tot}}} \cdot E_{\mathrm{kin}}(s), \quad (5)$$

where c_{l} is the aerodynamic lift coefficient. To account for the losses in the final drive under bi-directional power flow, we write (3) as two inequality constraints according to

$$\frac{\mathrm{d}}{\mathrm{d}s} E_{\mathrm{kin}}(s) \leq F_{\mathrm{m}}(s) \cdot \eta_{\mathrm{fd}} - F_{\mathrm{d}}(s) - F_{\mathrm{brake}}(s), \quad (6)$$

$$\frac{\mathrm{d}}{\mathrm{d}s} E_{\mathrm{kin}}(s) \leq F_{\mathrm{m}}(s) \cdot \frac{1}{\eta_{\mathrm{fd}}} - F_{\mathrm{d}}(s) - F_{\mathrm{brake}}(s), \quad (7)$$

where $F_{\mathrm{m}}(s)$ is the mechanical output force from the EM and η_{fd} is the efficiency of the final drive, assumed constant. Due to the objective (1), in case of traction, (6) will hold with equality, whilst in case of regenerative braking, (7) will hold with equality, thus capturing the bi-directional power flow.

The relation between the kinetic energy and velocity of the vehicle is defined by a convex relaxation as

$$\frac{1}{2} \cdot m_{\mathrm{tot}} \cdot v^2(s) \leq E_{\mathrm{kin}}(s) \leq \frac{1}{2} \cdot m_{\mathrm{tot}} \cdot v_{\mathrm{max}}^2(s), \quad (8)$$

where $v_{\mathrm{max}}(s)$ is the maximum velocity possible without exceeding the tire grip limitations on the race track. This maximum velocity profile can be pre-computed according to the method shown in [17].

In contrast to single-lap scenarios, a stint is represented by the vehicle starting and stopping at the pit box with a certain number of flying laps in between. However, since we are working in space domain, the lethargy would diverge to infinity for zero velocity. To solve this issue, we define a minimal velocity v_{min} close to standstill and enforce this value to the initial and final velocity with

$$E_{\mathrm{kin}}(0) = E_{\mathrm{kin}}(S_{\mathrm{stint}}) = \frac{1}{2} \cdot m_{\mathrm{tot}} \cdot v_{\mathrm{min}}^2. \quad (9)$$

When driving through the pit lane, the vehicle should adhere to a strict speed limit, of which the exact value is track-dependent. Therefore, we define an upper bound $v_{\mathrm{pit,max}}$ on the vehicle velocity when the vehicle is exiting or entering the pit as

$$E_{\mathrm{kin}}(s) \leq \frac{1}{2} \cdot m_{\mathrm{tot}} \cdot v_{\mathrm{pit,max}}^2 \quad \forall s \in \mathcal{S}_{\mathrm{pit}}, \quad (10)$$

where $\mathcal{S}_{\mathrm{pit}}$ is the set of distance-based positions that are part of the pit lane. Finally, we have to consider the maximum deceleration of the vehicle whenever the maximum velocity profile is not an active constraint, e.g., during braking before the pit entry. Assuming straight line braking, we can express the maximum deceleration as a lower bound on the kinetic energy with

$$\frac{\mathrm{d}E_{\mathrm{kin}}}{\mathrm{d}s}(s) \geq -F_{\mathrm{d}}(s) - \mu \cdot (m_{\mathrm{tot}} \cdot g + F_{\mathrm{down}}(s)), \quad (11)$$

where μ is the friction coefficient of the tires.

2.2. Electric machine

This section derives a convex representation of the operating limits and power losses of the EM. In general, we can distinguish between a maximum torque and maximum power operating region for an EM. Translating this to constraints in space domain results in a lower and upper bound on the mechanical output force of the EM for the maximum torque region as

$$F_{\mathrm{m}}(s) \in \left[-\frac{T_{\mathrm{m,max}} \cdot \gamma_{\mathrm{fd}}}{r_{\mathrm{w}}}, \frac{T_{\mathrm{m,max}} \cdot \gamma_{\mathrm{fd}}}{r_{\mathrm{w}}} \right], \quad (12)$$

where $T_{\mathrm{m,max}}$ is the maximum torque the EM can deliver, γ_{fd} is the final drive ratio and r_{w} is the radius of the rear wheels. Note that we include the final drive ratio, as we define the space-derivatives with respect to the vehicle reference frame. Similarly, the mechanical output force of the EM within the maximum power region is bounded as

$$F_{\mathrm{m}}(s) \in \left[-P_{\mathrm{m,max}} \cdot \frac{\mathrm{d}t}{\mathrm{d}s}(s), P_{\mathrm{m,max}} \cdot \frac{\mathrm{d}t}{\mathrm{d}s}(s) \right], \quad (13)$$

where $P_{\mathrm{m,max}}$ is the maximum power the EM can deliver.

We model the EM *force* losses $F_{\mathrm{m,loss}}(s)$ rather than the power losses as a function of the vehicle velocity and force of the EM. In general, an EM efficiency map shows large losses at low rotational velocities. Therefore, we want to include a term in our losses fit that is inversely proportional to the vehicle velocity. To ensure convexity, we model the EM losses as

$$F_{\mathrm{m,loss}}(s) = x_{\mathrm{m}}^{\top}(s) Q_{\mathrm{m}} x_{\mathrm{m}}(s), \quad (14)$$

where $x_{\mathrm{m}}(s) = \left[\frac{1}{\sqrt{v(s)}} \ \sqrt{v(s)} \ \frac{F_{\mathrm{m}}(s)}{\sqrt{v(s)}} \right]^{\top}$ and Q_{m} is a symmetric positive semi-definite matrix of coefficients, of which the values are determined through semi-definite programming. Fig. 3 shows the EM input force as a function of the EM output force and vehicle speed for the convex model and for the reference data. To implement the losses in a convex manner, we take the relation of the electrical EM input force $F_{\mathrm{ac}}(s)$ to the mechanical output force as

$$F_{\mathrm{ac}}(s) = F_{\mathrm{m}}(s) + F_{\mathrm{m,loss}}(s), \quad (15)$$

substitute the loss model, relax it and rewrite to a convex relaxation as

$$(F_{\mathrm{ac}}(s) - F_{\mathrm{m}}(s)) \cdot v(s) \geq y_{\mathrm{m}}^{\top}(s) Q_{\mathrm{m}} y_{\mathrm{m}}(s), \quad (16)$$

where $y_{\mathrm{m}}(s) = [1 \ v(s) \ F_{\mathrm{m}}(s)]^{\top}$.

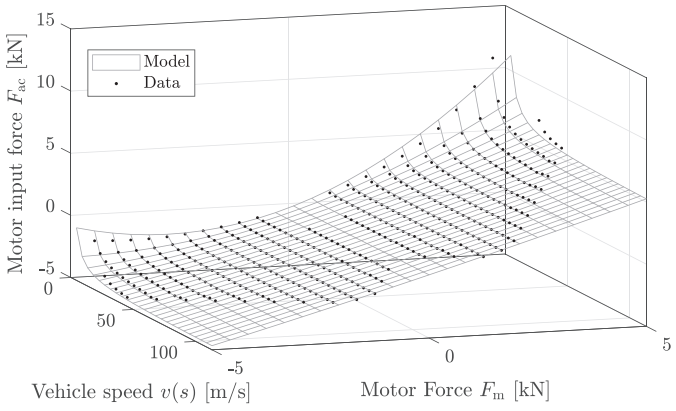

Fig. 3. A speed- and torque-dependent model of the EM. The normalized root-mean-square error (RMSE) of the model is 1.49% w.r.t. the maximum motor input force F_{ac}.

2.3. Inverter

In this section, we derive a quadratic model for the inverter losses. We apply the general quadratic power loss model of the form

$$P_{\mathrm{dc}}(s) = \alpha \cdot P_{\mathrm{ac}}^2(s) + P_{\mathrm{ac}}(s), \quad (17)$$

where α is an efficiency parameter, subject to identification. Converting this constraint to forces, rewriting and relaxing results in

$$(F_{\mathrm{dc}}(s) - F_{\mathrm{ac}}(s)) \cdot \frac{\mathrm{d}t}{\mathrm{d}s}(s) \geq \alpha \cdot F_{\mathrm{ac}}^2(s), \tag{18}$$

where $F_{\mathrm{dc}}(s)$ is the force equivalent to the electrical inverter input power.

2.4. Battery

This section derives a model for the battery efficiency and the power-split between the electrical inverter power and the auxiliary component power. The latter can be observed from Fig. 2 and is written as

$$P_{\mathrm{b}}(s) = P_{\mathrm{dc}}(s) + P_{\mathrm{aux}}, \tag{19}$$

where $P_{\mathrm{b}}(s)$ is the battery power at the terminals. Here, the auxiliary component supply is assumed to be constant and unidirectional, while the other powers are bi-directional. Converting (19) to forces results in

$$F_{\mathrm{b}}(s) = F_{\mathrm{dc}}(s) + P_{\mathrm{aux}} \cdot \frac{\mathrm{d}t}{\mathrm{d}s}(s), \tag{20}$$

where $F_{\mathrm{b}}(s)$ is the force equivalent of the battery power at the terminals.

The battery efficiency is mostly determined by its internal resistance R_0 and open-circuit voltage V_{oc}. We derive the battery losses from a Thévenin model [21] as

$$P_{\mathrm{l}}(s) = \frac{1}{P_{\mathrm{sc}}} \cdot P_{\mathrm{i}}^2(s) + P_{\mathrm{b}}(s), \tag{21}$$

where $P_{\mathrm{sc}} = \frac{V_{\mathrm{oc}}^2}{R_0}$ is the short-circuit power [22], which can be obtained from manufacturer data and which we assume to be constant. $P_{\mathrm{b}}(s)$ is the power at the battery terminals and $P_{\mathrm{l}}(s)$ is the internal battery power, which ultimately dictates a change in battery energy. Translating (21) to forces and relaxing results in

$$(F_{\mathrm{i}}(s) - F_{\mathrm{b}}(s)) \cdot \frac{\mathrm{d}t}{\mathrm{d}s}(s) \cdot P_{\mathrm{sc}} \geq F_{\mathrm{i}}^2(s), \tag{22}$$

where $F_{\mathrm{i}}(s)$ is the internal battery force and $F_{\mathrm{b}}(s)$ is the battery force at the terminals.

The energy consumption of the battery is modeled as

$$\frac{\mathrm{d}}{\mathrm{d}s}E_{\mathrm{b}}(s) = -F_{\mathrm{i}}(s). \tag{23}$$

We constrain the battery energy as

$$E_{\mathrm{b}}(0) = E_{\mathrm{b},0}, \tag{24}$$

$$E_{\mathrm{b,min}} \leq E_{\mathrm{b}}(s) \leq E_{\mathrm{b,max}}, \tag{25}$$

where $E_{\mathrm{b},0}$ is the initial battery energy. Furthermore, $E_{\mathrm{b,min}}$ and $E_{\mathrm{b,max}}$ correspond to the battery energy at the lower and upper State of Energy (SOE) bound, respectively. We leverage a lookup table with input charge time t_{charge} and output $E_{\mathrm{b},0}$ for a given charging profile during pre-processing.

2.5. Low-level optimization problem

This section presents the minimum-stint-time control problem of the electric race car. Given a predefined stint length and charge time we formulate the control problem using the state variables $x = (E_{\mathrm{kin}}, E_{\mathrm{b}})$ and the control variables $u = (F_{\mathrm{m}}, F_{\mathrm{brake}})$ as follows:

Problem 1 (Minimum-stint-time Control Strategy)**.** *The minimum-stint-time control strategies are the solution of*

$$\min \int_0^{S_{\mathrm{stint}}} \frac{\mathrm{d}t}{\mathrm{d}s}(s)\,\mathrm{d}s,$$

$$\text{s.t. } (2), (4) - (13), (16), (18), (20), (22) - (25).$$

Since the constraint set and the cost function are convex, the low-level control problem is fully convex and therefore we can compute the globally optimal solution with standard nonlinear programming methods.

3. High-level race optimization

In this section, we present the high-level maximum-race-distance control problem. First, we formulate the maximum-race-distance control problem that optimizes the stint length and charge time for a pre-defined number of pit stops. Second, we model the minimum stint time by leveraging the low-level control problem and optimizing for various combinations of stint length and initial battery energy. Finally, we extend the maximum-race-distance control problem to allow joint optimization of the stint length, charge time, and number of pit stops.

3.1. Mixed-integer control problem

We define the high-level control problem for a pre-defined number of pit stops in *stint domain*, so that we have a fixed and finite optimization horizon. Here, each index in the optimization variables represents a stint. The goal is then to maximize the driven distance as the sum of all completed laps during the stints as

$$\max S_{\mathrm{race}} = \max \sum_{k=0}^{N_{\mathrm{stops}}} S_{\mathrm{lap}} \cdot N_{\mathrm{laps}}(k), \tag{26}$$

where S_{race} is the total race distance, N_{stops} is the pre-defined number of pit stops, $N_{\mathrm{laps}}(k) \in \mathbb{N},\ \forall\ k \in \left[0, \ldots,\ N_{\mathrm{stops}}\ -\ 1\right]$ is the stint length and $\mathbb{N}$ the set of natural numbers, and S_{lap} is the length of one lap. Since the vehicle starts and stops at the pit box, the stint length should be an integer number of laps. As it is unlikely that the vehicle is exactly at the finish line when the race time limit is reached, we allow the final stint length to be a non-integer number of laps. This way, we have $N_{\mathrm{stops}} + 1$ stints for N_{stops} pit stops and thus we have N_{stops} integer stint lengths and one final non-integer stint length.

The race can be divided into the car driving a stint and recharging the battery during pit-stops. Given the total race time t_{race}, we can link it to the time to complete the stint $t_{\mathrm{stint}}(k) \geq 0$ and the time spent charging $t_{\mathrm{charge}}(k) \geq 0$ as

$$t_{\mathrm{race}} = \sum_{k=0}^{N_{\mathrm{stops}}} t_{\mathrm{stint}}(k) + \sum_{k=1}^{N_{\mathrm{stops}}} t_{\mathrm{charge}}(k). \tag{27}$$

We then decompose the total race into blocks consisting of a pit stop followed by a stint. By assuming that a stint is always energy limited, the charge time uniquely defines the initial battery energy for the subsequent stint and is not influenced by prior stints. To ensure that the battery is not overcharged, we apply an upper bound on the charge time through

$$t_{\mathrm{charge}}(k) \leq t_{\mathrm{charge,max}}, \tag{28}$$

where $t_{\mathrm{charge,max}}$ is the maximum charge time corresponding to a full battery, assuming that the battery is always charged starting from the lower energy bound. Since we start the race with a full battery, we set $t_{\mathrm{charge}}(0) = t_{\mathrm{charge,max}}$ and do not count it in the objective. Finally, the time to complete the stint is obtained by solving the low-level control problem, which we explain in the subsequent section.

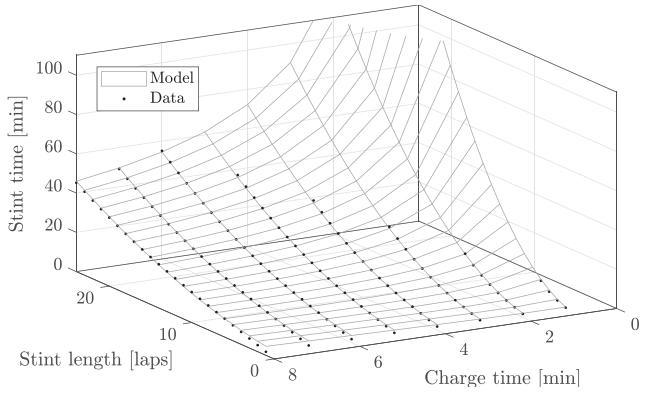

Fig. 4. Fit of optimization data for a combination of stint lengths and charge times. The normalized RMSE of the fit is 0.80 % w.r.t. the maximum stint time.

3.2. Stint time model

In this section, we derive a method for modeling the stint time as a function of the stint length and charge time during the pit stop prior to the stint. We solve the low-level control Problem 1 for a combination of stint lengths and initial battery energy to obtain the respective achievable minimum stint time. This way, we can create the lookup table with stint time as a function of stint length and charge time, as shown in Fig. 4. Thereby the charge time and initial battery energy are linked through a pre-defined charging current profile, cf. Section 2.4. As the stint time increases for larger stint lengths and shorter charge times, similar to the EM loss fit in Section 2.2 above, we approximate the low-level optimization results via the continuous function

$$t_{\text{stint}}(k) = x_{\text{s}}^{\top}(k) Q_{\text{s}} x_{\text{s}}(k), \tag{29}$$

where $x_{\text{s}}(k) = \left[\frac{1}{\sqrt{t_{\text{charge}}(k)}} \ \sqrt{t_{\text{charge}}(k)} \ \frac{N_{\text{laps}}(k)}{\sqrt{t_{\text{charge}}(k)}}\right]^{\top}$ and Q_{s} is a symmetric positive semi-definite matrix of coefficients. The result of the fit is shown in Fig. 4. For a convex implementation, we relax and rewrite (29) to

$$t_{\text{stint}}(k) \cdot t_{\text{charge}}(k) \geq y_{\text{s}}(k)^{\top} Q_{\text{s}} y_{\text{s}}(k), \tag{30}$$

where $y_{\text{s}}(k) = \left[1 \ t_{\text{charge}}(k) \ N_{\text{laps}}(k)\right]^{\top}$, and convert this relaxation to a conic constraint [23] as

$$t_{\text{stint}}(k) + t_{\text{charge}}(k) \geq \left\| \begin{matrix} 2 \cdot z_{\text{s}}(k) \\ t_{\text{stint}}(k) - t_{\text{charge}}(k) \end{matrix} \right\|_2, \tag{31}$$

where $z_{\text{s}} = C_{\text{s}} y_{\text{s}}(k)$ with C_{s} being the Cholesky factorization of Q_{s} [23]. Since it is optimal to minimize stint time, this constraint will hold with equality at the optimum.

3.3. Optimal pit stop strategy

In the previous sections, we introduced the objective and constraints for the high-level control problem when optimizing the race strategy for a pre-defined number of pit stops. In this section, we apply some modifications in order to jointly optimize the stint lengths, charge times and number of pit stops, thereby removing the need to search over a large space of pre-defined number of pit stops.

We define a binary variable $b_{\text{pit}}(k)$ that indicates whether pit stop and stint k is taken or skipped as

$$b_{\text{pit}}(k) = \begin{cases} 0, & \text{if stop and stint skipped} \\ 1, & \text{if stop and stint taken,} \end{cases} \tag{32}$$

and include it in (29) via the big-M formulation [24]

$$t_{\text{stint}}(k) \geq x_{\text{s}}(k)^{\top} Q_{\text{s}} x_{\text{s}}(k) - M \cdot (1 - b_{\text{pit}}(k)), \tag{33}$$

where $M \gg t_{\text{stint,max}}$. This way, we obtain the original constraint if $b_{\text{pit}}(k) = 1$ and we obtain a negative lower bound when $b_{\text{pit}}(k) = 0$ which, together with $t_{\text{stint}}(k) \geq 0$, will push the k-th stint time to zero, hence skipping the stint. We convert (33) to a cone as

$$M \cdot (1 - b_{\text{pit}}(k)) + t_{\text{stint}}(k) + t_{\text{charge}}(k) \geq \left\| \begin{matrix} 2 \cdot z_{\text{s}}(k) \\ M \cdot (1 - b_{\text{pit}}(k)) + t_{\text{stint}}(k) - t_{\text{charge}}(k) \end{matrix} \right\|_2. \tag{34}$$

Hence, whenever a stint is skipped, the corresponding stint time and charge time will be zero if an optimal solution is obtained. To prevent the stint length from diverging to infinity whenever the stint is actually skipped, i.e., $b_{\text{pit}}(k) = 0$, we define an upper bound on stint length as

$$N_{\text{laps}}(k) \leq N_{\text{laps,max}} \cdot b_{\text{pit}}(k), \tag{35}$$

where $N_{\text{laps,max}}$ is the maximum stint length that was used to obtain the lookup table. This will ensure $N_{\text{laps}}(k) = 0$ whenever $b_{\text{pit}}(k) = 0$. Finally, we enforce $b_{\text{pit}}(0) = 1$ since the first stint at the start of the race is always taken, and place driven stints first as

$$b_{\text{pit}}(k+1) \geq b_{\text{pit}}(k), \quad \forall k \in [1, N_{\text{stops}}] \tag{36}$$

3.4. High-level optimization problem

This section presents the maximum-race-distance control problem of the electric race car. Given a predefined race time we formulate the control problem using the control variables $(t_{\text{charge}}, N_{\text{laps}}, b_{\text{pit}})$ as follows:

Problem 2 (Maximum-race-distance Strategies)**.** *The maximum-race-distance strategies are the solution of*

$$\max \sum_{k=0}^{N_{\text{stops}}} S_{\text{lap}} \cdot N_{\text{laps}}(k),$$

$$\text{s.t. } (27), (28), (34) - (36).$$

Since Problem 2 can be solved with mixed-integer second-order conic programming solvers, we can guarantee global optimality upon convergence.

4. Discussion

A few comments are in order. First, we assume that endurance racing tires do not degrade significantly and can be changed every stint due to the long pit stop time. Yet the high-level control problem can be readily extended to capture these dynamics if the lookup table is devised accounting for tire degradation. Second, we assume that the time gained from starting the race from the grid compared to the pit lane is negligible on a full endurance race. Thus we do not separately optimize the first stint. Similarly, we do not separately optimize the final stint, since we assume that the vehicle can push the SoE below the lower limit to complete the final lap of the race, as battery degradation would no longer be an issue. Third, we assume that the cooling system can cope with the requested power from the battery and EM and devote temperature modeling to future research. Yet again, the high-level control problem can capture temperature effects if the map is devised accounting for the temperatures and by assuming that the temperatures at the start of the stint are always the same. Finally, it might occur that the vehicle can recuperate more energy, compared to what is needed to drive to the pit box, during braking before pit entry. Yet this amount of energy can be neglected, since it does not affect the PO and stint time.

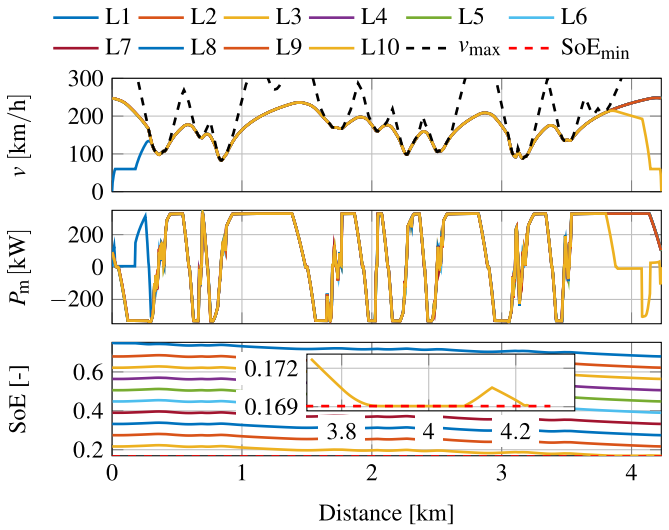

Fig. 5. Velocity, EM power and battery SoE trajectories per lap for a 10 lap stint. The battery energy is an active constraint, thus the stint is energy limited. The EM power shows a gradual decrease at high velocities, thus indicating energy management. The zoom window corresponds to the final 500 m of the stint.

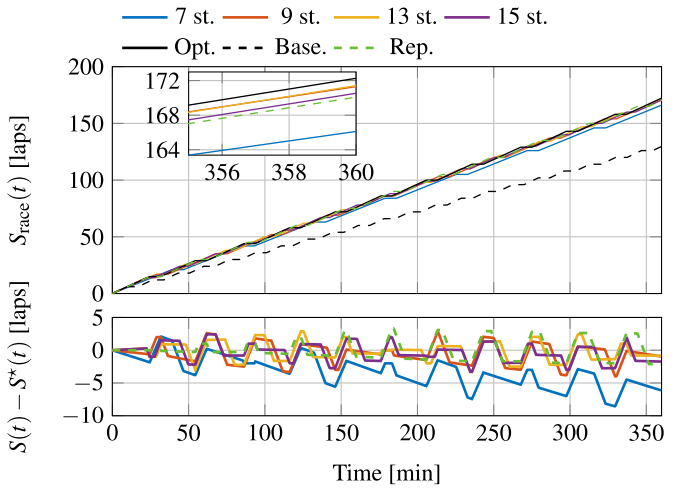

Fig. 6. Evolution of the completed laps as a function of time for the optimal strategy (black) and the strategies optimized for a fixed number of pit stops. The dashed data show a baseline strategy and a repetition strategy of the global optimal stint. The zoom window corresponds to the final 5 min of the race and illustrates the difference in race distance between the optimized strategies, showing that jointly optimizing the number of stints can significantly outperform other strategies by multiple laps.

5. Results

This section presents numerical results for both the low- and high-level control problem. We base our use case on the electric endurance race car of InMotion [25], shown in Fig. 1, performing a 10 lap stint at the Zandvoort circuit for the low-level control problem and a 6 h race at the same circuit for the high-level control problem. First, we discuss the numerical solutions for both control problems. Second, we validate the high-level control problem by comparing the optimal race strategy against fixed-pit-stop-number strategies and calculate the theoretical optimal combinations of stint length and charge time.

For the discretization of the model, we apply the Euler Forward method except for the lethargy, where we apply the trapezoidal method, with a fixed step-size of $\Delta s = 4$ m. We parse the low-level control problem with CasADi [26] and solve it using IPOPT [27] combined with the MA57 linear solver [28], whilst we parse the high-level control problem with YALMIP [29] and solve it using MOSEK [30]. We perform the numerical optimization on an Intel Core i7-4710MQ 2.5 GHz processor and 8 GB of RAM. Thereby, the computation time for solving the low-level problem was about 4.6 s of parsing and 25 s of solving, whereas the high-level problem needed 0.04 s of parsing and 0.57 s of solving.

5.1. Low-level optimization

In this section, we compute the optimal trajectories for a stint of 10 laps around the Zandvoort circuit. We set the initial battery capacity to the upper bound corresponding to a 7.5 min charge time. The total stint time is about 946 s with an average flying lap time of 93 s.

The velocity profile together with the EM power and SoE per lap is shown in Fig. 5. First, we observe that the velocity profiles of consecutive free-flow laps are equivalent, as there are no lap-dependent dynamics. Second, the EM power decreases gradually before the vehicle reaches a corner and full regenerative braking is applied, which defines the optimal PO. Finally, we observe that the pit lane speed limit is adhered to, but the power at pit exit and pit entry are slightly different. From the lower plot, we notice that the lower battery limit is reached before the end of the stint, indicating that the recuperated energy during pit entry is larger than the required energy for driving through the pit lane. However, this does not affect the stint time or the PO.

5.2. High-level optimization

This section presents the optimal race strategy in terms of number of pit stops, stint length and charge time, and we compare it against the strategies optimized for a fixed number of pit stops. We select a 6 h race, yet longer races can be solved as well with our approach, considering the very low computational times needed by our high-level framework to converge. To link the initial battery energy $E_{b,0}$ to the charge time t_{charge}, we apply constant current charging starting from the lower limit.

Fig. 6 shows the evolution of the completed laps as a function of time for various fixed-pit-stop-number strategies. We observe that the optimal strategy of 11 stops results in the largest number of completed laps, thereby confirming that it is indeed optimal in terms of number of pit stops. The difference in covered race length between the optimal and fixed-pit-stop-number strategies can exceed multiple laps and hence significantly affect the final race outcome in terms of finishing position, highlighting the importance of jointly optimizing the number of pit stops. Furthermore, we compare the optimal race strategy against a strategy that repeats the global optimal stint of 15 laps and 7.5 min charging, until the race ends. Although the stints used in this strategy are globally optimal from a stint perspective, it does not cover the largest distance within the 6 h time window, which makes the strategy sub-optimal from a race perspective. This is because a pure repetition of the optimal stint does not fit perfectly within the 6 h race. Instead, it is beneficial to slightly deviate from the optimal stint, so that the stints fit better within the race, as done by the optimal race strategy. This shows that the optimal race strategy is not necessarily the same as the optimal stint, thereby highlighting the importance of jointly optimizing the stint lengths, charge times and number of pit stops. Lastly, to show the importance of the bi-level approach, we compare the optimal strategy against a baseline *flat-out* strategy whereby no energy management is applied to limit energy consumption, but the EMs are rather operated at maximum power whenever possible. This results in 6lap stints and a total race distance of 132 laps, whilst the globally optimal

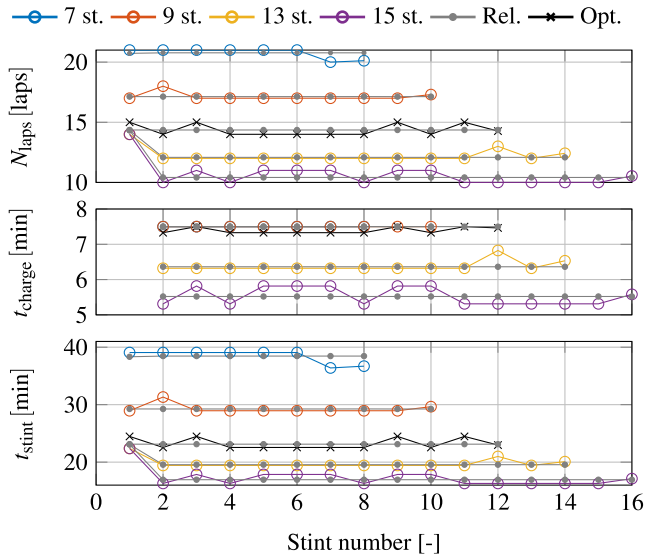

Fig. 7. Optimal race strategy (black) in terms of stint length, charge time and stint time with $t_{charge,max} = 7.5\,min$. For comparison, we show other optimal fixed pit stops strategies together with the relaxed solution in gray. Stint length, charge- and stint time are related and the optimal integer solution minimizes the differences to the relaxed solution.

solution is about 172 laps, which is about 30 % better compared to the baseline.

Fig. 7 shows the individual stints in terms of length and charge time, together with the relaxed non-integer solution. We can conclude that a constant stint length over the race is optimal, since all stints in the relaxed solutions are equal, with the only exception being the first stints. In this use case, the optimal integer solution consists of the stint lengths that minimize the difference to the relaxed solution, namely, of a stint length between 14 and 15 laps together with a charge time of almost 7.5 min and 11 pit stops in total. For strategies with more stops, both the stint lengths and charge times are reduced, thus showing that partly charging the battery is optimal for more than 11 stops. For strategies with fewer than 11 stops, the charge time is already maximized and no compensation is possible for increasing stint lengths. From the aforementioned observations, we conclude that the stint length, stint time and charge time are closely related in the case of an optimal solution. Thereby, all the stints consist of a unique and lap-wise equal globally optimal PO.

5.3. Validation

In this section, we validate the numerical combinations of stint length and charge time for the various strategies. To this end, we calculate the average stint velocity $\overline{v}_{stint}(k)$ for every strategy as

$$\overline{v}_{stint}(k) = \frac{S_{stint}(k)}{t_{charge}(k) + t_{stint}(k)}, \quad \forall k > 0. \tag{37}$$

Arguably, the globally optimal stint should maximize the average stint velocity. Fig. 8 shows the average stint velocity for all possible combinations of stint length and charge time together with the theoretical optimal charge times that maximize the average stint velocity for a given stint length, to which we refer as the optimal combinations. These optimal combinations show an almost linear relation between charge time and stint length until the maximum charge time is reached. The globally optimal stint consists of 15 laps and 7.5 min charging, which is the exact same combination that we obtained as the optimal strategy in the previous

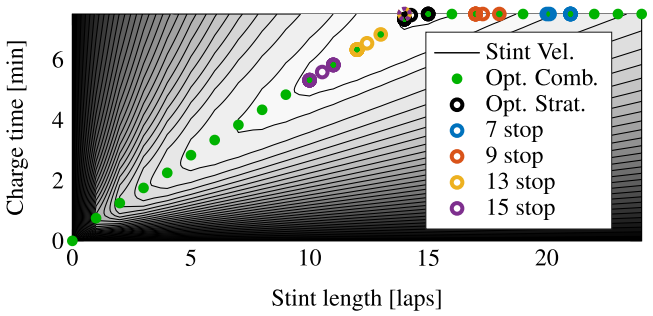

Fig. 8. The average stint velocity for a combination of stint length and charge time together with the optimal combinations and actual numerical solutions. The optimal combinations of stint length and charge time show a clear (linear) correlation, to which the numerical solutions are aligned. The dashed circles indicate the first stints for the 13 and 15 stop strategies.

section. Furthermore, we observe that the average stint velocity decreases in sensitivity around the optimal combinations for increasing stint length and charge time, until the maximum charge time is reached. Thereby, increasing the stint length beyond 15 laps quickly becomes less favorable, explaining why the 7 stop strategy is significantly worse than the others. Finally, we note that the numerical solutions align well with the theoretically optimal combinations. The outliers at 14 laps and 7.5 min charging correspond to the first stints, for which the charge time is not part of the race and thus the calculation of the stint velocity in (37) is not valid.

6. Conclusion

In this paper, we devised a bi-level optimization framework to efficiently solve the maximum-distance endurance race strategy problem for a fully electric race car. In order to tackle the large problem size stemming from the length of an endurance race, we decomposed the problem into separate stints which we solved by extending a minimum-lap-time convex optimization framework that can rapidly deliver the globally optimal solution to account for multiple laps and include more accurate force-based models. This way, we were able to compute the optimal number of pit stops, the charging time per stop and the individual stint lengths via mixed-integer second-order conic programming with global optimality guarantees. Our bi-level framework could solve the problem of a 6 h race around the Zandvoort circuit with low computation times below 1 s for the high-level framework. Our results showed that, from a stint perspective, there is a clear correlation between optimal stint length and charge time, which corresponds to the maximization of the average stint velocity. Moreover, the optimal race strategy showed a 30 % increase in the overall race distance, compared to a baseline flat-out strategy. Finally, we highlighted the importance of optimizing both levels and that, compared to the strategies optimized for a pre-defined number of pit stops, jointly optimizing the number of pit stops can significantly increase the total distance driven by multiple laps, hence considerably improve the achievable race outcome.

This work opens the field for the following possible extensions: First, we want to account for the temperature dynamics of the EM and the battery during driving and charging, since they can play an important role in endurance racing scenarios [10,18]. Second, we want to study the impact of the vehicle dynamics [9,31] and tire degradation on the achievable stint time and the resulting race strategies.

Declaration of Competing Interest

The authors declare that they have no known competing financial interests or personal relationships that could have appeared to influence the work reported in this paper.

Acknowledgment

We thank Dr. I. New, Ir. S. Broere and Ir. M. Konda for proofreading, and G. Delissen for the photograph. This paper was partly supported by the NEON research project (project number 17628 of the Crossover program which is (partly) financed by the Dutch Research Council (NWO)).

References

[1] FIA, 2021 fia world endurance championship: Sporting regulations, 2021, Available online at https://www.fia.com/sites/default/files/2021_wec_sporting_regulations_-_wmsc161220-clean_1.pdf.
[2] R. Lot, S. Evangelou, Lap time optimization of a sports series hybrid electric vehicle, in: World Congress on Engineering, 2013.
[3] T. Sedlacek, D. Odenthal, D. Wollherr, Minimum-time optimal control for battery electric vehicles with four wheel-independt drives considering electrical overloading, in: Vehicle System Dynamics, 2020.
[4] D. Casanova, On minimum time vehicle manoeuvring: The theoretical optimal lap, in: Cranfield University, 2000. Ph.D. thesis
[5] D. Limebeer, G. Perantoni, Optimal control for a formula one car with variable parameters, Vehicle System Dynamics 52 (5) (2014) 653–678.
[6] F. Christ, A. Wischnewski, A. Heilmeier, B. Lohmann, Time-optimal trajectory planning for a race car considering variable tyre-road friction coefficients, Vehicle System Dynamics 59 (2019) 588–612, doi:10.1080/00423114.2019.1704804.
[7] N.D. Bianco, R. Lot, M. Gadola, Minimum time optimal control simulation of a gp2 race car, Journal of Automobile Engineering 232 (2017) 1180–1195, doi:10.1177/0954407017728158.
[8] A. Heilmeier, A. Wischnewski, L. Hermansdorfer, J. Betz, M. Lienkamp, B. Lohmann, Minimum curvature trajectory planning and control for an autonomous race car, Vehicle System Dynamics 58 (10) (2020) 1497–1527.
[9] T. Herrmann, F. Christ, J. Betz, M. Lienkamp, Energy management strategy for an autonomous electric racecar using optimal control, in: Proc. IEEE Int. Conf. on Intelligent Transportation Systems, 2019. doi:10.1109/ITSC.2019.8917154
[10] T. Herrmann, F. Passigato, J. Betz, M. Lienkamp, Minimum race-time planning-strategy for an autonomous electric racecar, in: Proc. IEEE Int. Conf. on Intelligent Transportation Systems, 2020.
[11] X. Liu, A. Fotouhi, D. Auger, Optimal energy management for formula-e cars with regulatory limits and thermal constraints, Applied Energy 279 (2020).
[12] T. Herrmann, F. Sauerbeck, M. Bayerlein, M. Betz, J.a. Lienkamp, Optimization-based real-time-capable energy strategy for autonomous electric race cars, in: SAE International Journal of Connected and Automated Vehicles In press, 2021.
[13] X. Liu, A. Fotouhi, Formula-e race strategy development using artificial neural networks and monte carlo tree search], Neural Computing and Applications volume 32 (2020) 15191–15207, doi:10.1007/s00521-020-04871-1.
[14] S. Ebbesen, M. Salazar, P. Elbert, C. Bussi, C.H. Onder, Time-optimal control strategies for a hybrid electric race car, IEEE Transactions on Control Systems Technology 26 (1) (2018) 233–247.
[15] M. Salazar, P. Elbert, S. Ebbesen, C. Bussi, C. H. Onder, Time-optimal control policy for a hybrid electric race car, IEEE Transactions on Control Systems Technology 25 (6) (2017) 1921–1934.
[16] P. Duhr, G. Christodoulou, C. Balerna, M. Salazar, A. Cerofolini, C.H. Onder, Time-optimal gearshift and energy management strategies for a hybrid electric race car, Applied energy 282 (115980) (2020).
[17] O. Borsboom, C.A. Fahdzyana, T. Hofman, M. Salazar, A convex optimization framework for minimum lap time design and control of electric race cars, IEEE Transactions on Vehicular Technology 70 (9) (2021) 8478–8489.
[18] A. Locatello, M. Konda, O. Borsboom, T. Hofman, M. Salazar, Time-optimal control of electric race cars under thermal constraints, European Control Conference (2021).
[19] A. Heilmeier, M. Graf, M. Lienkamp, A race simulation for strategy decisions and circuit motorsports, in: Proc. IEEE Int. Conf. on Intelligent Transportation Systems, 2018.
[20] W.J. West, D.J.N. Limebeer, Optimal tyre management for a high-performance race car, Vehicle System Dynamics 231 (2020) 1–19.
[21] L. Guzzella, A. Sciarretta, Vehicle propulsion systems: Introduction to Modeling and Optimization, 2nd, Springer Berlin Heidelberg, 2007.
[22] O. Borsboom, C.A. Fahdzyana, M. Salazar, T. Hofman, Time-optimal control strategies for electric race cars for different transmission technologies, in: IEEE Vehicle Power and Propulsion Conference, 2020.
[23] S. Boyd, L. Vandenberghe, Convex optimization, Cambridge Univ. Press, 2004.
[24] A. Richards, J. How, Mixed-integer programming for control, in: American Control Conference, 2005.
[25] InMotion, InMotion fully electric LMP3 car, 2022, Available online at https://www.inmotion.tue.nl/en/about-us/cars/revolution.
[26] J.A.E. Andersson, J. Gillis, G. Horn, J.B. Rawlings, M. Diehl, Casadi – a software framework for nonlinear optimization and optimal control, Mathematical Programming Computation 11 (1) (2019) 1–36.
[27] A. Wachter, L.T. Biegler, On the implementation of an interior-point filter line-search algorithm for large-scale nonlinear programming, Mathematical Programming 106 (1) (2006) 25–57.
[28] HSL, A collection of fortran codes for large scale scientific computation, http://www.hsl.rl.ac.uk.
[29] J. Löfberg, YALMIP : A toolbox for modeling and optimization in MATLAB, in: IEEE Int. Symp. on Computer Aided Control Systems Design, 2004.
[30] MOSEK ApS, MOSEK Optimization Toolbox for MATLAB 9.3.20, 2019. [Online] Available: https://docs.mosek.com/latest/toolbox/index.html.
[31] S. Broere, M. Salazar, Minimum-lap-time control strategies for all-wheel drive electric race cars via convex optimization, in: European Control Conference, 2022. In press. Available online at https://arxiv.org/abs/2111.04650